High curvatures drive river meandering

Zoltán Sylvester *[1], Jacob Covault †[1], and Paul Durkin ‡[2]

[1]Bureau of Economic Geology, The University of Texas at Austin
[2]University of Manitoba

Abstract

One of the long- and widely held ideas about the dynamics of meandering rivers is that migration slows down in bends with higher curvatures. Identifying the radius of curvature at which migration is fastest is standard practice in field studies of meandering rivers. High-resolution measurements of local migration rates in time-lapse Landsat images from two rapidly migrating rivers in the Amazon Basin suggest that the variation of migration rate closely follows that of the local curvature, with a roughly constant phase lag between the two; and a quasi-linear relationship exists between curvature and migration rate if this lag is taken into account. A simple numerical model of meandering illustrates the link between curvature and migration rate and reproduces observations from the studied rivers. The implication is that meandering rivers migrate fastest at, and slightly downstream of, locations of high curvature; and one of the most important ways river migration is rejuvenated and meandering patterns are reshuffled is the generation of high-curvature bends through cutoffs.

Introduction

Meandering rivers are among the most dynamic sedimentary systems on Earth. Meander bends of large rivers, especially ones with a high sediment discharge, can migrate several meters per year [1]. Understanding and predicting how meanders change through time has major implications for a number of engineering and geological problems, including management of agricultural land, loss of infrastructure, bridge design, and distribution of heterogeneities in porous sediments and sedimentary rocks. The meandering process consists of erosion on the outer bank and deposition on the inner bank, which are the result of an asymmetric distribution of flow velocity and shear stress in curved channel segments [2]. Inertial forces drive the high-velocity core of the river towards the outer bank; the strength of this effect is dependent on the bend curvature [3]. In theory, the larger the curvature (1/R), or smaller the radius of curvature (R), the larger the centrifugal force and the shear stress exerted on the outer bank. Therefore, bends with high curvature should also have the highest migration rates. However, early studies of the relationship between curvature and migration rate suggested that migration rate reaches its highest value when the radius of curvature is about two to three times the width of the river (W) [4; 5; 6]. High-curvature bends with an R/W value of less than two appeared to migrate more slowly, potentially due to an increase in energy loss and the development of a separation zone on the upstream side of the bend [4; 7]. In parallel with these field measurements, theoretical and numerical modeling work has shown that the velocity excess at the outer bank depends not only on the local curvature, but it is a function of the weighted sum of upstream curvatures [8; 7; 9].

*corresponding author, zoltan.sylvester@beg.utexas.edu
†jake.covault@beg.utexas.edu
‡pdurkin@ucalgary.ca

Although it has been suggested that migration rate is a monotonic function of curvature if bend length is taken into account [9], the idea that high-curvature bends show limited migration persists and is frequently explored in field studies, despite the increasing scatter in the plot of migration rate versus R/W as more data points are added [10; 11; 12]. High curvatures also seem to be associated with low migration rates in numerical modeling results [13].

Although significant progress has been made recently in understanding the impact of sediment discharge on bend-averaged migration rates between different rivers [1] and as a result of cutoffs [14], the bend-scale variability of migration rates has received limited attention. Time-lapse satellite imagery provides an opportunity to re-evaluate the relationship between curvature and migration rate at a temporal and spatial resolution that was not possible before. Our hypothesis is that migration rate is a monotonic function of curvature [9] and that high-curvature bends undergo rapid migration. To test this hypothesis, we have digitized channel centerlines from Landsat images of two rivers in the Amazon Basin and estimated local migration rates using dynamic programming, a technique that is often used to correlate two time series (e.g., [15]). Then we used a simple model of meandering [7] to investigate the local curvature - migration rate relationship and compare modeled distributions of curvature and migration rates with the field data.

Curvature and migration rates in the Mamore and Ucayali rivers

Rivers of the Amazon Basin that drain the Andes have high water and sediment discharges and are among the fastest migrating meandering rivers on Earth [1]. Here we focus on two segments of the Mamore and Ucayali rivers, segments that are unaffected by a strong variation in cut-bank erodibility; that is, there are no obvious locations where the river would be in contact with bedrock or significantly older alluvium. The Landsat images used for the analysis of the Mamore River were taken about three years apart (on November 6, 1986 and July 9, 1989), whereas those covering the Ucayali River were taken two years apart (on August 13, 1987 and August 26, 1989). Channel centerlines were digitized manually and local curvatures and migration rates were estimated along the resampled centerlines.

In order to compare two variables with the same units, we use the concept of 'nominal migration rate' instead of curvature (Figure 1; [7]). This is the migration rate that would be expected if migration was only a function of local curvature and it is the product of the dimensionless curvature (W/R) and the erodibility constant k_l [7]:

$$R_0 = k_l \frac{W}{R} \tag{1}$$

The erodibility constant can be estimated from the actual migration rate, as the weighted sum of upstream curvatures should match the measured migration rates.

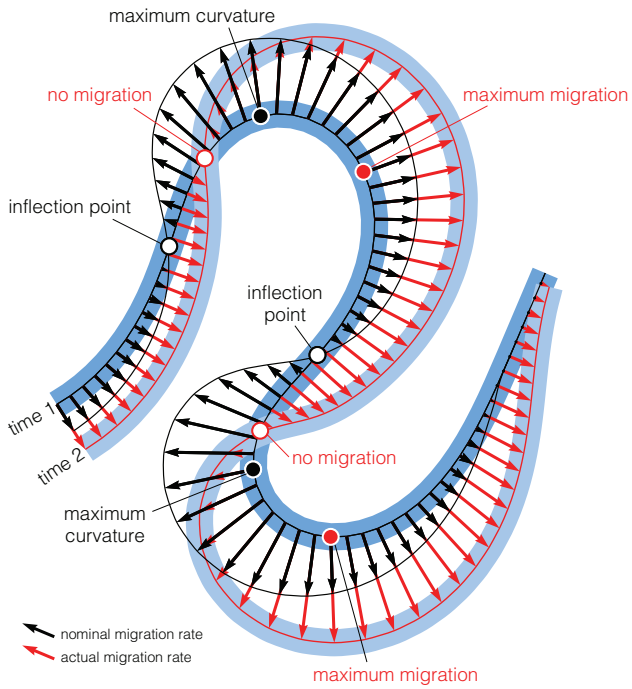

Figure 1: Nominal (black arrows) and actual (red arrows) migration rates plotted along two modeled meander bends, showing downstream delay of the maximum actual migration rate relative to maximum bend curvature.

Results from both river segments show strong similarities between the variation of curvature and the migration rate (Figures 2A,B and 3A,B). As expected, there is a lag between curvature and migration rate, with points of maximum migration being consistently located downstream from points of maximum curvature. The magnitude of this lag shows a relatively low variability, across bends of different sizes and curvatures, and can be estimated by computing correlation coefficients between nominal and actual migration rates and finding the lag for which the correlation is the highest (Figure 2D). For the Mamore River, the lag is ˜570 m; for the Ucayali River, its value is ˜1500 m. These values are slightly larger than twice the channel width.

Using these lags to shift the curves, nominal and actual migration rates show a linear correlation (r-squared values of 0.70 and 0.66 for the Mamore and Ucayali rivers, respectively; Figures 2E and 3D). This correlation would break down if we did not consider the phase lag between curvature and migration rate.

Actual migration rates can be predicted using the Howard and Knutson (1984) [7] approach:

$$R_1(s) = \Omega R_0(s) + \left(\Gamma \int_0^\infty R_0(s-\xi)G(\xi)d\xi\right)\left(\int_0^\infty G(\xi)d\xi\right)^{-1}, \tag{2}$$

where Ω and Γ are weighting parameters with values of -1 and 2.5, and $G(\xi)$ is a weighting function:

$$G(\xi) = e^{\alpha\xi}, \tag{3}$$

where α is a function of friction factor C_f and water depth D:

$$\alpha = k2C_f/D. \tag{4}$$

The predicted migration rates match relatively well the measured migration rates, with r-squared values of 0.69 and 0.65 (Figures 2F and 3E). The mismatch between nominal and actual, as well as predicted and

actual migration rates seems to increase at larger values, but there is no indication that actual migration rates would decrease beyond a critical high curvature.

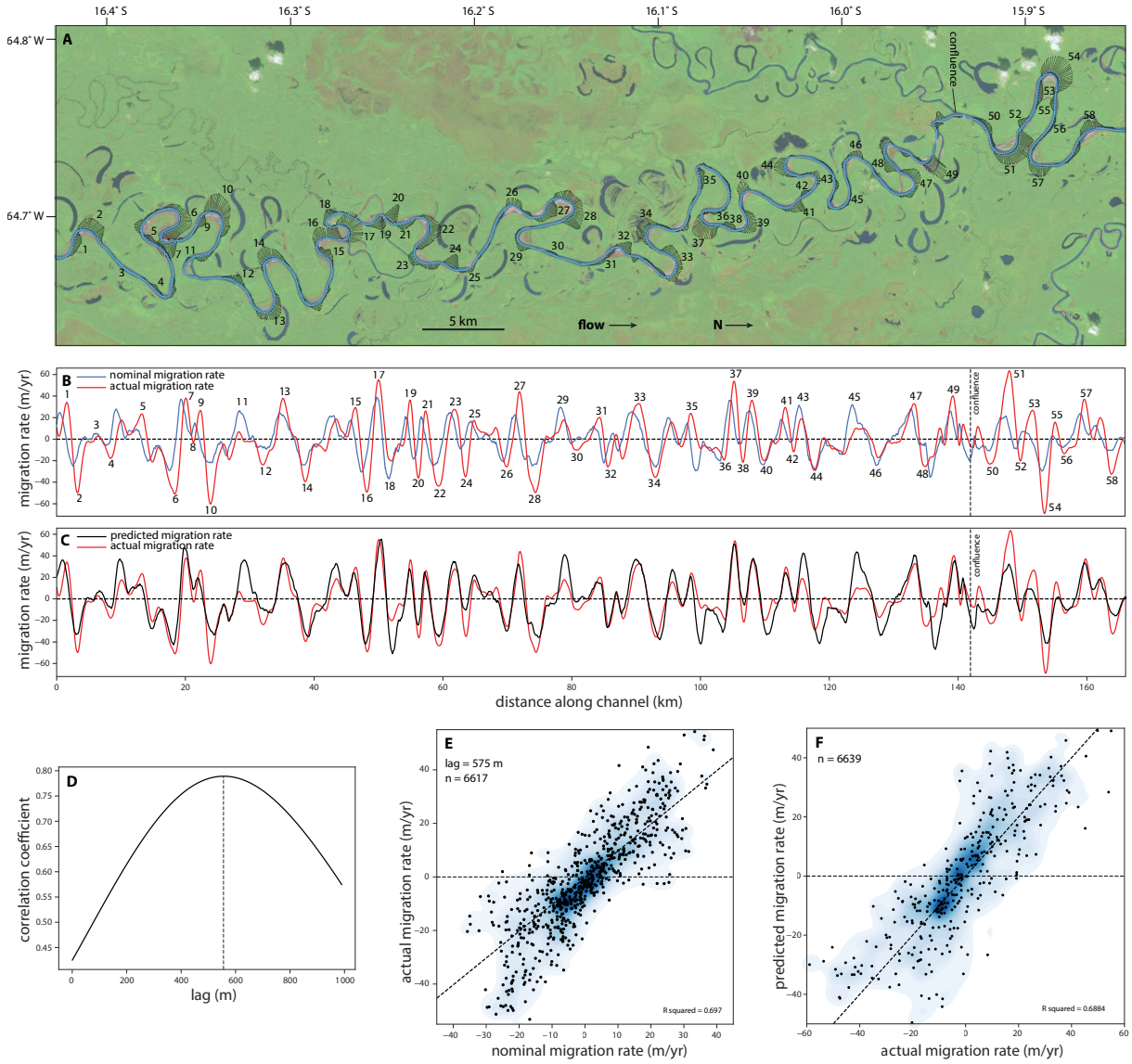

Figure 2: Analysis of channel migration of the Mamore River, Bolivia, over a three year period. (A) Landsat image from 1986, with local migration rate vectors plotted. Bend numbers correspond to those shown in (B). (B) Along-channel variation of nominal migration rate and actual migration rate. (C) Plot of predicted and actual migration rates. Prediction is based on an erodibility constant of 60 m/yr and a friction factor of 0.009. (D) Variation of the correlation coefficient between actual and nominal migration rates as a function of the lag correction applied. (E) Kernel density estimate plot of actual and nominal migration rates. Dashed line corresponds to one-to-one line. Only a fraction of the data points are shown in scatterplot. (F) Kernel density estimate plot of predicted and actual migration rates. Dashed line corresponds to one-to-one line. Only a fraction of the data points are shown in scatterplot.

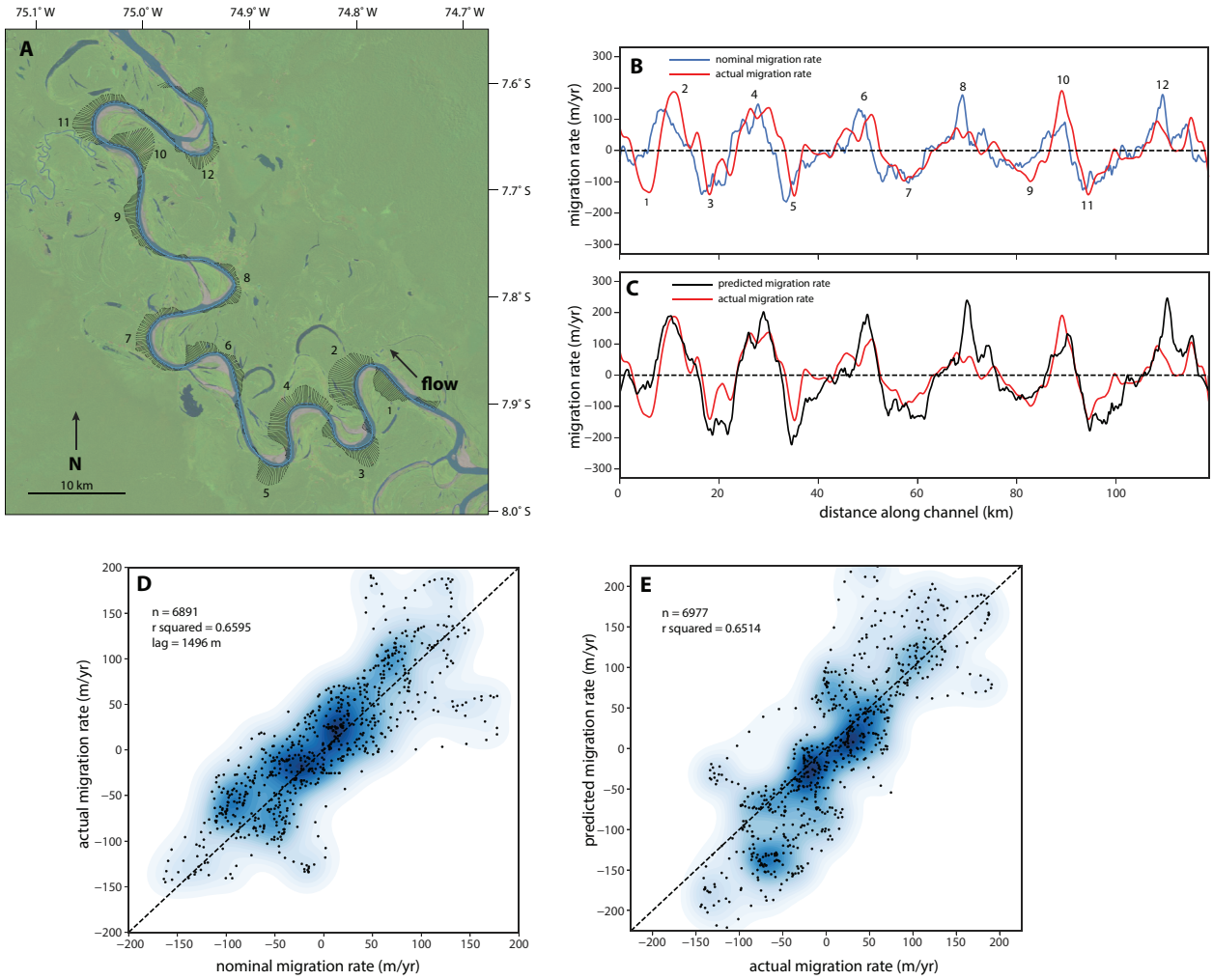

Figure 3: Analysis of channel migration of the Ucayali River, Peru, over a two year period. (A) Landsat image from 1987, with local migration rate vectors plotted. Bend numbers correspond to those shown in (B). (B) Along-channel variation of nominal migration rate and actual migration rate. (C) Plot of predicted and actual migration rates. Prediction is based on an erodibility constant of 300 m/yr and a friction factor of 0.007. (D) Kernel density estimate plot of actual and nominal migration rates. Dashed line corresponds to one-to-one line. Only a fraction of the data points are shown in scatterplot. (E) Kernel density estimate plot of predicted and actual migration rates. Dashed line corresponds to one-to-one line. Only a fraction of the data points are shown in scatterplot.

Bend-averaged curvatures and migration rates of the Mamore River, estimated using an approach similar to previous studies [4], largely plot within the envelope of Nanson and Hickin (1986) [6] (Figure 4). However, the analysis above shows that the apparent decrease in migration rates at small values of R/W is an artifact of not correcting for the phase lag between the two. Local, high-resolution measurements of curvature should be matched with migration rate values at one lag distance downstream from the point of interest. Bend-averaged curvatures, averaged between two inflection points, should be compared to average migration rates between two consecutive points of no migration that are located downstream from the first inflection point of the meander bend (Figure 1).

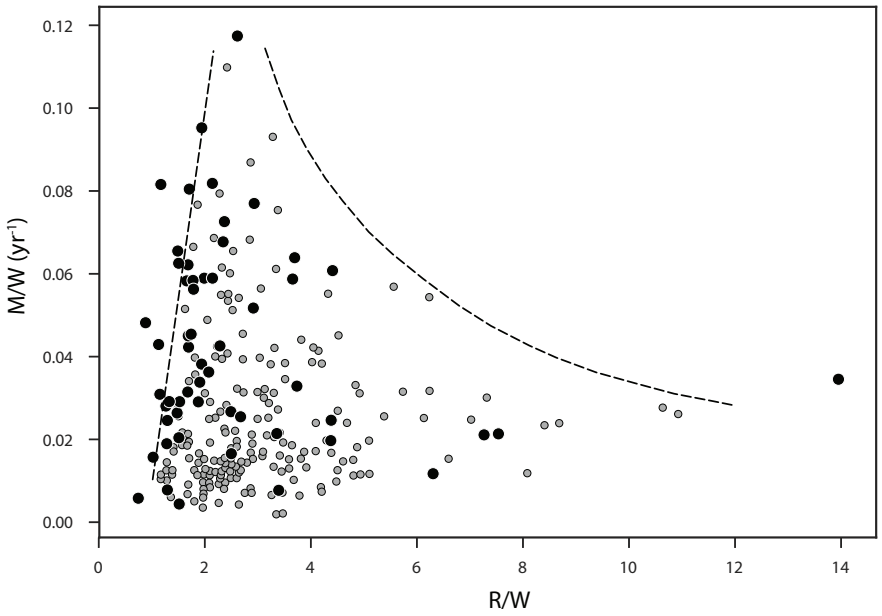

Figure 4: Plot of normalized bend-averaged migration rate (M/W) against dimensionless radius of curvature (R/W) for the Mamore River segment shown in Figure 2A. Smaller grey dots in background and dashed-line envelope are from Nanson and Hickin (1986)

Results from a simple model of meandering

To better understand the linkages between curvature and migration rate observed in the studied river segments, we have used an implementation of the simplest numerical model of meandering [7]. Although the starting point for this model is the Hickin and Nanson (1975) [4] relationship between R/W and migration rate, we have used a simple linear dependence of the nominal migration rate on the local curvature, an approach similar to 'case 1' in [7]. Model parameters were tuned so that the inputs and outputs approximately match the parameters estimated for the Mamore River (Figure 5).

If the model runs long enough so that the initial regular series of meanders is replaced by bends with highly variable geometry, the output becomes visually similar to the highly sinuous Mamore and Ucayali rivers. This is especially the case if point bar deposits in the model are gradually covered by vegetation and older oxbow lakes disappear due to filling (Figure 5B). As expected from the model setup, nominal and actual migration rates vary in tandem and they are offset by a lag that shows limited variability (Figure 5C), just like in the case of the field data. Plotting local migration rate against R/W we get a point cloud that resembles the bend-averaged plots of Nanson and Hickin (1986) [6]; this could be interpreted as decreasing migration rates at low values of R/W (see also [13]). However, if we consider the lag between curvature and migration rate, the data points collapse onto a hyperbola (Figure 5E). As actual migration rate and curvature seem to correlate in a quasi-linear fashion, it is more insightful to plot migration rate against dimensionless curvature (W/R; Figure 5F). This plot is analogous to plots of nominal and actual migration rates (Figures 2E, 3D).

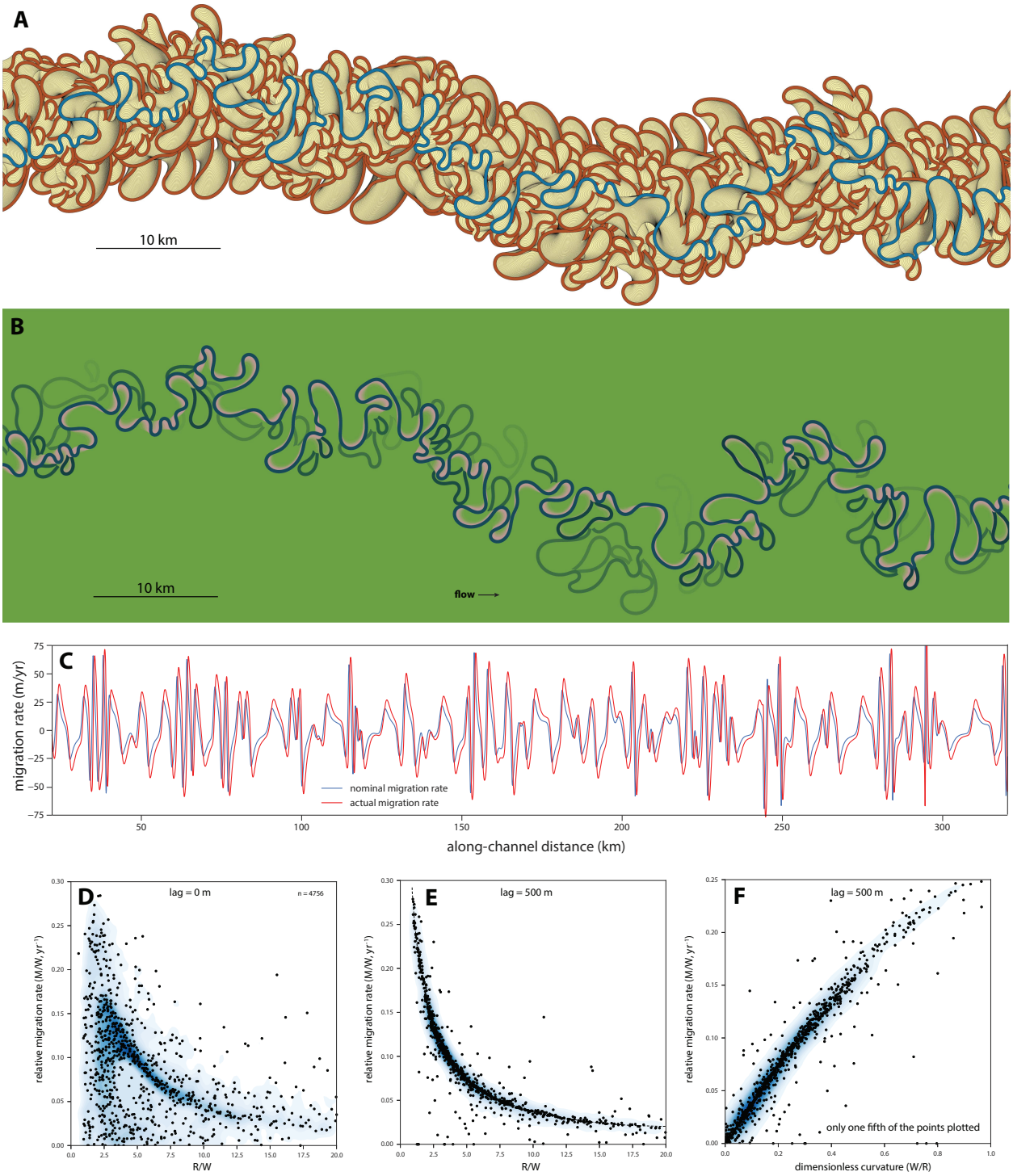

Figure 5: Results from a simulation based on a linear dependence of migration rate on curvature. (A) Output of a long-term simulation, using input parameters tuned to match the Mamore River. Most recent channel shown in blue, point bar deposits are yellow, and oxbow fills are brown. (B) Same output as in (A), but showing only point bars younger than 15 years and oxbows younger than 70 years. (C) Plot of nominal and actual migration rates as a function of along-channel distance. (D) Plot of normalized migration rate against R/W, showing a point cloud similar to that of Nanson and Hickin (1986). (E) Same plot as in (D), but the lag between curvature and migration rate is taken into account. (F) Plot of absolute migration rate against dimensionless curvature, corrected for a 500 m lag.

Implications for river meandering

Previous work has demonstrated the importance of considering upstream curvatures when estimating migration rates [8; 7; 9; 16]. Significant progress has also been made in highlighting the impact of high-order terms and nonlinearity on meander bend morphology and long-term evolution [17; 16; 18], as well as the importance of variations in bank erodibility [19; 20; 21]. Recent studies have also shown how migration rates are influenced by changes in sediment discharge [1; 14]. Our results suggest that the link between meander curvature and migration rate is relatively simple and raise the possibility that the understanding and prediction of several aspects of river migration can be improved using simple linear models like that of Howard and Knutson (1984) [7].

To summarize our findings, high-resolution estimates of channel migration along two large, rapidly migrating rivers in the Amazon Basin suggest that (1) there is a quasi-linear relationship between local curvature and migration rate and (2) locations of maximum curvature and maximum migration are separated by a roughly constant lag which is about twice the river width. Contrary to the widely held idea that channel migration slows down at high curvatures, we find that the sharpest bends are the ones that migrate with the highest speed. Channel widening and flow separation are likely to be the result of rapid downstream migration, not the cause of an apparent drop in migration rate. One of the important implications of the relationship between high curvatures and high migration rates is that meander cutoffs play a key role in rejuvenating river migration. Increased migration rates up- and downstream from cutoff locations have been linked to increased sediment discharge [14]. Our results suggest that high curvatures generated at cutoffs play a role as well: most meanders start out after a cutoff event as small, rapidly migrating sharp bends that later undergo a slower expansion associated with lower curvatures. The abundance of medium-curvature bends [3] is probably the result of the short-lived nature of sharp bends with high migration rates.

Methods

Centerline interpretation was performed manually, using georeferenced Landsat images, downloaded from the EarthExplorer USGS website (`https://earthexplorer.usgs.gov/`). Point spacing along centerlines was about half the channel width. We have used Jupyter notebooks ([22]; `http://jupyter.org/`) to perform the data analysis and modeling. Channel centerlines were resampled using B-spline interpolation so that distances between consecutive points are about equal and close to one quarter of the channel width. Curvature was computed at every point along the centerline using Cartesian coordinates:

$$C = \frac{x'y'' - y'x''}{(x'^2 + y'^2)^{3/2}}, \tag{5}$$

where x' and x'' denote first and second derivatives of the x coordinate. The result was smoothed using the Savitzky-Golay filter [23]. To estimate migration rates, we used a Python implementation of the dynamic time warping algorithm (available at `https://github.com/dpwe/dp_python`), which is often applied to correlate two time series of different lengths (Figure 6). In this case, we minimized the distance between points along the two centerlines. Some points on the first centerline will have two matching points on the second centerline; in cases like this we considered only one of the distances. This approach slightly underestimates the migration rate when the channel movement did not take place along the shortest path.

Next, the nominal migration rate is estimated:

$$R_0 = k_l W C, \tag{6}$$

where k_l is the migration rate constant, W is channel width and C is curvature. The migration rate constant (or erodibility) is not known, but can be estimated knowing that the actual migration rate is slightly larger than the nominal migration rate: for a bend with constant curvatures and without any weighting, equation (2) simplifies to $R_1 = 1.5R_0$, so we know that $R_1 > R_0$ and $R_1 < 1.5R_0$.

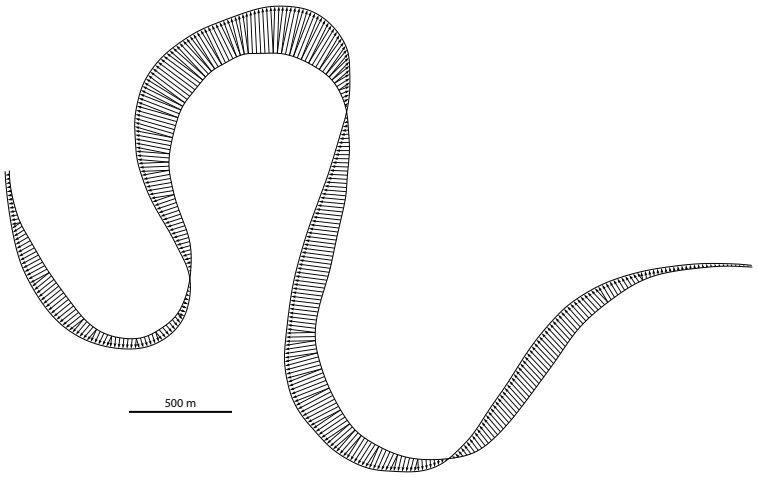

Figure 6: Migration vectors between two centerlines. Links between points established through dynamic time warping.

Once the nominal migration rate is known, it can be compared with the actual migration rate, and the phase lag can be estimated through applying linear regression to the two variables, using varying lags (Figure 2D). We can also estimate the actual migration rate with equation (2) and compare this predicted value with the measured one (Figures 2C,2F, 3C,3E). To do this, we have estimated river widths from the satellite images and used the following regression between width and depth [24]:

$$W = 18.8D^{1.41}. \tag{7}$$

The friction factor C_f needs to be fine-tuned so that the actual migration rate is matched when using equations (2) and (4). We have found that values of 0.005-0.01 give realistic results.

For the numerical modeling of meander evolution, we have used a Python implementation of the Howard and Knutson (1984) model [7] (see also [25]). This approach is based on an empirical relationship between migration rate and curvature and no flow velocities are computed. However, the formulation used here is equivalent to the Howard and Knutson (1984) model [8] and it is computationally efficient, with a small number of parameters. The key difference relative to previous implementations is that the nominal migration rate is a simple function of curvature and there is no critical curvature value beyond which this relationship is reversed (equation 6). Neck cutoffs are identified and executed whenever the distance between non-neighboring centerline points becomes less or equal to one channel width.

Model results were displayed either in a stratigraphic format, where all preserved channel segments, including oxbow fills, are visible, regardless of age (Figure 5A); or in a geomorphologic format, where point bars and oxbow fills older than a certain age are covered by vegetation (Figure 5B).

Code is available from first author upon request.

Acknowledgements

We are thankful for support by sponsors of the Quantitative Clastics Laboratory (`http://www.beg.utexas.edu/qcl`) and for discussions with Richard Sech, Brian Willis, Tao Sun, Kaveh Gayour, Nick Howes, and Matt Wolinsky.

References

[1] J. A. Constantine, T. Dunne, J. Ahmed, C. Legleiter, and E. D. Lazarus. Sediment supply as a driver of river meandering and floodplain evolution in the Amazon Basin. *Nature Geoscience* **7**, 899–903 (2014).

[2] W. E. Dietrich, J. D. Smith, and T. Dunne. Flow and Sediment Transport in a Sand Bedded Meander. *The Journal of Geology* **87**, 305–315 (1979).

[3] L. B. Leopold and M. G. Wolman. River meanders. *Geological Society of America Bulletin* **71**, 769–794 (1960).

[4] E. J. Hickin and G. C. Nanson. The Character of Channel Migration on the Beatton River, Northeast British Columbia, Canada. *Geological Society of America Bulletin* **86**, 487–494 (1975).

[5] G. C. Nanson and E. J. Hickin. Channel Migration and Incision on the Beatton River. *Journal of Hydraulic Engineering* **109**, 327–337 (1983).

[6] G. C. Nanson and E. J. Hickin. A statistical analysis of bank erosion and channel migration in western Canada. *Geological Society of America Bulletin* **97**, 497–504 (1986).

[7] A. D. Howard and T. R. Knutson. Sufficient conditions for river meandering: A simulation approach. *Water Resources Research* **20**, 1659–1667 (1984).

[8] S. Ikeda, G. Parker, and K. Sawai. Bend theory of river meanders. Part 1. Linear development. *Journal of Fluid Mechanics* **112**, 363–377 (1981).

[9] D. J. Furbish. River-bend curvature and migration: How are they related? *Geology* **16**, 752–756 (1988).

[10] D. Knighton. Fluvial forms and processes: a new perspective. Arnold (1998).

[11] P. F. Hudson and R. H. Kesel. Channel migration and meander-bend curvature in the lower Mississippi River prior to major human modification. *Geology* **28**, 531–534 (2000).

[12] J. Hooke. Complexity self-organisation and variation in behaviour in meandering rivers. *Geomorphology* **91**, 236–258 (2007).

[13] A. Crosato. Physical explanations of variations in river meander migration rates from model comparison. *Earth Surface Processes and Landforms* **34**, 2078–2086 (2009).

[14] J. Schwenk and E. Foufoula-Georgiou. Meander cutoffs nonlocally accelerate upstream and downstream migration and channel widening. *Geophysical Research Letters* **43**, 12437–12445 (2016).

[15] L. E. Lisiecki and P. A. Lisiecki. Application of dynamic programming to the correlation of paleoclimate records. *Paleoceanography* **17**, 1–12 (2002).

[16] I. Gneralp and B. L. Rhoads. Empirical analysis of the planform curvature-migration relation of meandering rivers. *Water Resources Research* **45**, 1–15 (2009).

[17] A. Frascati and S. Lanzoni. Morphodynamic regime and long-term evolution of meandering rivers. *Journal of Geophysical Research* **114(F2)**, 1–12 (2009).

[18] J. Schwenk and E. Foufoula-Georgiou. Are process nonlinearities encoded in meandering river planform morphology? *Journal of Geophysical Research: Earth Surface* **122**, 1534–1552 (2017).

[19] T. Sun, P. Meakin, T. Jssang, and K. Schwarz. A Simulation Model for Meandering Rivers. *Water Resources Research* **32** 2937–2954 (1996).

[20] I. Gneralp and B. L. Rhoads. Influence of floodplain erosional heterogeneity on planform complexity of meandering rivers. *Geophysical Research Letters* **38**, 1–6 (2011).

[21] M. Bogoni, M. Putti, and S. Lanzoni. Modeling meander morphodynamics over self-formed heterogeneous floodplains. *Water Resources Research* **53**, 5137–5157 (2017).

[22] T. Kluyver, B. Ragan-Kelley, F. Prez, B. E. Granger, M. Bussonier, J. Frederic, K. Kelley, J. Hamrick, J. Grout, S. Corlay, P. Ivanov, D. Avila, S. Abdalla, and C. Willing. Jupyter Notebooks-a publishing format for reproducible computational workflows. In F. Loizides and B. Schmidt, editors, *Positioning and Power in Academic Publishing Players, Agents and Agendas*, 87–90. IOP Press (2016).

[23] A. Savitzky and M. J. E. Golay. Smoothing and Differentiation of Data by Simplified Least Squares Procedures. *Analytical Chemistry* **36**, 1627–1639 (1964).

[24] K. Konsoer, J. Zinger, and G. Parker. Bankfull hydraulic geometry of submarine channels created by turbidity currents: Relations between bankfull channel characteristics and formative flow discharge. *Journal of Geophysical Research: Earth Surface* **118**, 216–228 (2013).

[25] Z. Sylvester and J. A. Covault. Development of cutoff-related knickpoints during early evolution of submarine channels. *Geology* **44**, 835–838 (2016).